Clim. Past Discuss., 9, 1449–1483, 2013
www.clim-past-discuss.net/9/1449/2013/
doi:10.5194/cpd-9-1449-2013

Climate of the Past Discussions
Open Access

A comparative study of large scale atmospheric circulation in the context of future scenario (RCP4.5) and past warmth (Mid Pliocene)

Y. Sun[1,2,3], **G. Ramstein**[3], **C. Contoux**[3,4], **and T. Zhou**[1,5]

[1]LASG, Institute of Atmospheric Physics, Chinese Academy of Sciences, Beijing, China
[2]University of Chinese Academy of Sciences, Beijing, China
[3]Laboratoire des Sciences du Climat et de l'Environnement/IPSL, UMR8212, CEA-CNRS-UVSQ, Gif-sur-Yvette, France
[4]Université Pierre et Marie Curie & CNRS, Sisyphe, Paris, France
[5]Climate Change Research Center, Chinese Academy of Sciences, Beijing, China

Received: 21 February 2013 – Accepted: 6 March 2013 – Published: 20 March 2013

Correspondence to: G. Ramstein (gilles.ramstein@lsce.ipsl.fr),
Y. Sun (sunyong@mail.iap.ac.cn)

Published by Copernicus Publications on behalf of the European Geosciences Union.

Abstract

The Pliocene climate (3.3 ~ 3.0 Ma) is often considered as the last sustained warm period with close enough geographic configurations compared to the present one and associated with atmospheric CO_2 concentration (405 ± 50 ppm) higher than the modern level. It is therefore suggested that the warm Pliocene climate may provide a plausible scenario for the future climate warming with the important advantage, that for mid-Pliocene, many marine and continental data are available. To investigate this issue, we selected RCP4.5 scenario, one of the current available future projections, to compare the pattern of tropical atmospheric response with past warm mid-Pliocene climate.

We performed three OAGCM simulations (RCP4.5 scenario, mid-Pliocene and present day simulation) with the IPSL-CM5A model and investigated atmospheric tropical dynamics through Hadley and Walker cell responses to warmer conditions. Our results show that there is a damping of the Hadley cell intensity in the northern tropics and an increase in both subtropics. Moreover, northern and southern Hadley cells expand poleward. The response of Hadley cell is stronger for RCP4.5 scenario than for mid-Pliocene, but in very good agreement with the fact the atmospheric CO_2 concentration is higher in future scenario than mid-Pliocene (543 versus 405 ppm). Concerning the response of the Walker cell, we showed that, despite very large similarities, there are also some differences. i.e. the common features are for both scenarios: weakening of the ascending branch, leading to a suppression of the precipitation over the western tropical Pacific. The response of Walker cell is stronger in RCP4.5 scenario than mid-Pliocene but also depicts some major difference as an eastward shift of the rising branch of Walker cell in future scenario compared to the mid-Pliocene.

In this paper, we explain the dynamics of the Hadley and Walker cell, and show that despite minor discrepancy, mid-Pliocene is certainly an interesting analogue for future climate changes in the tropical areas.

CPD
9, 1449–1483, 2013

1 Introduction

The mid-Pliocene warm period (~3 million years ago; 3 Ma), is known as the most recent period in Earth's history when the global average temperature was warmer than the present day for a sustained time (~300 thousand years) (Haywood et al., 2000; Haywood and Valdes, 2004). Despite there is some important differences in the height of mountain ranges that may for instance change high latitude temperature in Northern Hemisphere (Foster et al., 2010). Unlike other old geological warm periods, geographic distribution of continents and oceans for mid-Pliocene was the same as or very similar to the present one (Dowsett, 2006). During that period, CO_2 values are estimated to have reached 360–440 ppm and sea level was at least 22 ± 10 m above the modern levels (Krantz, 1991; Dowsett et al., 1992; Raymo et al., 1996; Miller et al., 2012). Given the availability of relatively large sets of palaeoenvironmental proxy data, it has therefore made mid-Pliocene as an unequalled "palaeo-analogue" for future climate predictions by the end of 21st century (Thompson and Fleming, 1996; Jansen et al., 2007).

Indeed, future environmental scenarios and model predictions cannot be tested by observational data. However, looking at geological analogues, we can use the past environment as a guide for the understanding of future climate change and a test of the validity of climate models. The most recent warm climate associated to higher CO_2 value than modern is the mid-Pliocene; thereby there is no other way to learn about warm climate than to study on deep past climates that are geologically different from present-day one except mid-Pliocene (Salzmann et al., 2008). To better understand the dynamical causes for the mid-Pliocene warmth, and to further assess the ability of the climate models in simulating the past warm climate, a suite of simulations have been conducted for the mid-Pliocene warm period under the frame of the Pliocene Paleoclimate Modeling Intercomparison Project (PlioMIP). According to the PlioMIP, two experimental designs are required for each participating model. PlioMIP experimental designs are well documented in previous literature (Haywood et al., 2010, 2011).

CPD
9, 1449–1483, 2013

Previously, there have been long-term efforts in reconstructed global SST dataset (Dowsett et al., 1996; Dowsett and Robinson, 2009), which are very useful to validate PlioMIP simulations and further document the possible cause of the mid-Pliocene warm climate by modeling studies. However, how far mid-Pliocene represents what may happen during the 21st century? We shall focus here on tropical-subtropical atmospheric dynamics analysis in the mid-Pliocene and future climate to investigate the response of Hadley and Walker cells to the past and future warm climates.

Previous modeling studies reveal that the simulated mid-Pliocene global annual surface air temperature and global mean sea surface temperature are warmer compared with pre-industrial control experiment (Zhang et al., 2012). This past almost global warming have been well reproduced by the most recent modeling studies using the multi-coupled models and corresponding atmospheric components proposed by PlioMIP (Bragg et al., 2012; Contoux et al., 2012; Kamae and Ueda, 2012; Stepanek and Lohmann, 2012; Zhang and Yan, 2012; Haywood et al., 2013). The increase of surface air temperature is non-uniform, with the most significant heating at higher latitudes. As it has been shown (Masson-Delmotte et al., 2006), the greenhouse gases climate do show a polar amplification (i.e. decrease of equator-to-pole temperature gradient). Therefore cooling or warming leads to an increase or reduced temperature gradient that modulated the Hadley cell intensity and extent (Ramstein et al., 1998). Nevertheless, we also pointed out here that tropical atmospheric dynamics is very sensitive to this reduced temperature gradient. Reconstruction of sea surface temperature (SST) depicts a permanent El Niño-like condition over the tropical Pacific in mid-Pliocene, characterized by reduced east-west asymmetry in SST and subsurface thermocline depth (Wara et al., 2005; Ravelo et al., 2006). Some features of the atmospheric general circulation in the mid-Pliocene have been also investigated using AGCM simulation. A recent study suggests one of the key aspects of the mid-Pliocene climate is a slow-down of Walker circulation (Kamae et al., 2011), resulting from reduced east-west gradient of SST in the tropics, particularly in the Pacific Ocean and Indian Ocean. Subsequent analysis using idealized SST experiments pointed out the ascending branch

CPD
9, 1449–1483, 2013

of Hadley cell in both hemispheres expands poleward in mid-Pliocene warm period and the width of ascending branch is defined as the range between equator and maximum of MSF at 500 hPa. This widening in the southern cell is larger than that in the northern cell. The ascending branch of Hadley cell expands poleward in response to the warmer SST in higher latitude (Kamae et al., 2011).

As discussed above, most previous studies focused on mechanisms responsible for the mid-Pliocene warmth. The increasing importance of mid-Pliocene as an analogue of future climate warming induced by greenhouse gas is highlighted by the IPCC AR4 (Jansen et al., 2007). Thus the aim of the present study is to investigate whether mid-Pliocene represents a plausible comparative climate for atmospheric circulations changes in future scenario. Here, we depict not only the similarity of Hadley cell and Walker circulation produced by mid-Pliocene and future projection, but also pinpoint the differences and find out possible dynamical explanations for this differences between both simulations.

The structure of the present paper is organized as follows. A brief description of the model and experimental designs for past and future simulations is given in Sect. 2. In Sects. 3 and 4, we describe the comparative analysis of Hadley and Walker circulation between RCP4.5 simulation and mid-Pliocene climate relative to the pre-industrial experiment. Indeed, RCP4.5 is current moderate scenario available for present comparison with mid-Pliocene warm climate. Similarities and differences in the response of Hadley and Walker cells changes to global mid-Pliocene and future warm climate are discussed in Sect. 5. The impact of the Hadley and Walker circulation changes in both climates on precipitation is discussed in Sect. 6. Summary and general discussions conclude this study in the Sect. 7.

CPD
9, 1449–1483, 2013

2 Model description and experiment design

2.1 Model description

The model used for the present study is the last version of IPSL model (IPSL-CM5A) (Dufresne et al., 2012). This model is an earth system model developed by Institute Pierre Simon Laplace and currently used for past and future climate projections (Contoux et al., 2012; Dufresne et al., 2012). The four-component models are coupled together using OASIS3 coupler (Valcke 2006). The atmospheric model (LMDZ5A) has two standard resolutions: the low resolution is 1.875° (latitude) × 3.75° (longitude) with 39 vertical levels (96 × 96L39) and the mid-resolution is 1.25° (latitude) × 2.5° (longitude) with 39 vertical levels (143 × 144L39) (Hourdin et al., 2013). The ocean model version is NEMOv3.2 (182 × 149L31) and mean grid spacing is about 2° with latitudinal resolution of 0.5° near the equator and 1° in the Mediterranean Sea and 31 vertical levels in the ocean with 10 levels in the top 100 m (Madec, 2008). The land surface model used is ORCHIDEE (Organizing Carbon and Hydrology In Dynamic Ecosystems), consisting of three modules: hydrology, carbon cycle and vegetation dynamics (Krinner et al., 2005). The sea-ice model used here is LIM2 (Louvain-la-Neuve Sea Ice Model) (Fichefet and Maqueda, 1997).

IPSL-CM5A is an Earth system model based on an improved version of the IPSL-CM4 coupled ocean-atmosphere GCM that was used in CMIP3. Compared with IPSL-CM4, IPSL-CM5A includes the following improvements (Dufresne et al. 2012): (i) an increase vertical resolution of the atmosphere from 19 to 39 vertical levels, with 15 levels above 20 km (ii) six different species of aerosols that can be either externally prescribed or computed on-line (iii) stratospheric and tropospheric ozone can be either prescribed or computed on-line (iv) improved physical parameterizations of the ocean (v) carbon cycle models for both the ocean part and terrestrial part and land use change can be externally imposed.

Given different resolution versions of IPSL model (IPSL-CM5A-LR and IPSL-CM5A-MR) participation on the CMIP5 projection, our analysis is nevertheless based on the

CPD
9, 1449–1483, 2013

results from IPSL-CM5A-LR due to the fact that this resolution is used in the PlioMIP Intercomparison project (Contoux et al., 2012). Details of IPSL-CM5A model are available in previous studies (Marti et al., 2010).

2.2 Pre-industrial experimental design

Pre-industrial experiment is performed as required by CMIP5/PMIP3 by the LSCE modeling group. Greenhouse gases, solar constant and orbital parameters are set to pre-industrial values recommended by CMIP5/CMIP3. Solar constant is 1365 $W\,m^{-2}$, CO_2 and CH_4 concentrations are fixed 280 ppm and 760 ppb, respectively.

2.3 Mid-Pliocene warm period simulation

Recently, PlioMIP was established to assess the ability of various climate models in simulating the mid-Pliocene warm period as part of the PlioMIP (Haywood et al., 2010, 2011). Numerous modeling studies have been conducted for the mid-Pliocene warm period. The IPSL-CM5A-LR model participated in PlioMIP Intercomparison project. We performed fixed inherent ocean boundary and our results are in good agreement with data globally and depict the same main features as other AOGCM models involved in PlioMIP (Contoux et al., 2012). The mid-Pliocene warm period is performed by IPSL-CM5A-LR model and the boundary conditions for this coupled simulation are set following the PlioMIP experiment guidelines (Haywood et al., 2010, 2011). Modern coastline is employed in this simulation due to the challenge of changing the land-sea mask in the ocean model. According to PlioMIP, differences between mid-Pliocene and modern topographies are accounted by PRISM group adding as anomalies to IPSL-CM5A-LR model topography (Haywood et al., 2010, 2011). Imposed ice-sheet and vegetation reconstructions are derived from PRISM3. The orbital configuration, solar constant, greenhouse gases and aerosols were specified as similar to the pre-industrial control run except for atmospheric CO_2 concentration fixed at 405 ppm.

CPD
9, 1449–1483, 2013

2.4 Future climate projections

According to CMIP5 experiment design, the future projections are required for each participating model under the representative concentration pathways (RCPs) proposed by CMIP5, RCPs represent pathways of radiative forcing (in $W\,m^{-2}$) that reach a specific value by the end of 21st century relative to pre-industrial condition. There are four RCP scenarios: RCP2.6 (low), RCP4.5 (medium), RCP6.0 (medium-high) and RCP8.5 (high). The radiative forcing level of RCP2.6 scenario first reaches a value around $3.1\,W\,m^{-2}$ at the middle of 21st century, returning to $2.6\,W\,m^{-2}$ by 2100. Unlike the RCP2.6 sceario, RCP4.5 and RCP6.0 are stabilized scenarios and total radiative forcing is stabilized at $4.5\,W\,m^{-2}$ and $6.0\,W\,m^{-2}$ by 2100, respectively. RCP8.5 is quite different from other three scenarios characterized by a progressive increase total radiative forcing over the 21st century, peaking at $8.5\,W\,m^{-2}$ in 2100. Indeed, RCP4.5 is current moderate scenario available for present comparison with mid-Pliocene warm climate. The integration length of RCP4.5 scenario is almost 300 yr, from 1 January 2006 to 31 December 2300. The atmospheric CO_2 concentrations have been increasing and stabilize at 543 ppm in 2150. To investigate the robustness of the Hadley cell in the future scenario simulated by IPSL-CM5A-LR model, the other six model simulations (MPI-ESM-LR, BCC-CSM1.1, NorESM1-M, NCAR-CCSM4, FGOALS-S2, MIROC-ESM) from the Fifth Assessment Report (AR5) of the Intergovernmental Panel on Climate Change (IPCC) for RCP4.5 scenario are used for comparative analysis.

Here, we analyze the large scale atmospheric circulation produced by RCP4.5 and compare it with mid-Pliocene warm period. However, previous studies argued that mid-Pliocene should not be considered as an analogue for the present warming because the present warming represents a non-equilibrium perturbation of the climate system, whereas past warmth were probably closer to their equilibrium response to changes in external forcing (Crowley, 1996). It is possible that ocean processes in response to CO_2 increase are still not equilibrated due to the large inertia of ocean. We here will

CPD
9, 1449–1483, 2013

consider the fast atmospheric tropical response and choose the last 50 yr of the 300 yr' RCP4.5 simulation used for comparison with mid-Pliocene.

3 Changes of Hadley circulation in the RCP4.5 and mid-Pliocene compared to Pre-industrial control run

Mass stream function (hereafter MSF) is probably the most frequently used indicator to depict the Hadley circulation. Positive (negative) values of MSF indicate net northward (southward) mass transport (Oort and Yienger, 1996). As shown in Fig. 1a–b, we first examine annual averaged MSF derived from RCP4.5 and mid-Pliocene warm period. Hadley circulation consists in two enclosed Hadley cells, one is in the Northern Hemisphere (northern Hadley cell) and the other is in the Southern Hemisphere (southern Hadley cell). The latter is stronger than the former with respect to the strength and coverage. These features mentioned above can also be seen in the pre-industrial control simulation (not shown).

Important changes of Hadley circulation can be found in future projection relative to control run (Fig. 1c). Hadley circulation in the future scenario is characterized by weakening Hadley cell in the tropics and strengthening Hadley cell in the subtropics. Hadley circulation also depicts significant changes in mid-Pliocene in comparison with the control run (Fig. 1d). Coherent intensification occurs on the southern Hadley cell in mid-Pliocene, while Hadley cell in Northern Hemisphere has obvious regional changes associated with weakening of Hadley circulation in the northern tropics (equator-20° N) and intensified Hadley circulation in northern subtropics.

Despite there are many similarities on Hadley circulation in both warm climates when compared to pre-industrial control run, i.e. the strength of Hadley cell has obvious intensification in the both subtropics and decrease in the northern tropics. However, large differences still exist between the RCP4.5 and mid-Pliocene as displayed in Fig. 1e. The strength of Hadley circulation in RCP4.5 scenario is weakened in the tropics and enhanced in the subtropics of both hemispheres compared with that in the mid-Pliocene

CPD
9, 1449–1483, 2013

warm period and this difference would be contributed to the different behavior of Hadley cell boundaries between both simulations.

The strength of Hadley circulation derived from past and future warm climate are enhanced in subtropical regions of both hemispheres, which would have substantial influence on the boundaries of Hadley circulation. MSF at 500hPa is chosen to quantitatively illustrate the changes of the Hadley cell boundaries in both simulations relative to control run (Fig. 1f). Hadley cell boundaries are identified as the latitudes where the MSF equals 0 $Kg\,s^{-1}$. The latitudinal positions where the values of MSF are zero in both subtropical regions shift poleward in both warm climates, resulting from the intensified MSF in the subtropics compared with control run. Widening of Hadley cell also can be confirmed using another measurement of Hadley circulation as the vertical shear of meridional velocity (v250 minus v850) shown in the Fig. 2a (Quan et al., 2004).

Figure 2b quantifies the edge-latitudes of northern and southern Hadley cells, derived from the definition of MSF. Statistical analysis suggests that width of the southern Hadley cell is 1.9° southward whereas the northern Hadley cell is 0.8° northward expansion in the RCP4.5 simulation. This expansion simulated by RCP4.5 scenario also can be found in the mid-Pliocene, with 0.6° S shift poleward for southern Hadley cell twice as large as northern Hadley cell expansion (0.3° N) (Fig. 2c). The poleward expansion of Hadley cell edges are captured by both the future and past warm climates, but with different magnitude. I.e. the Hadley cell boundaries have significant poleward shift in the future climate compared with mid-Pliocene, together with 1.3° S and 0.5° N poleward expansion for southern and northern Hadley cell, respectively (Fig. 2d).

Multi-model comparison studies suggest properties of Hadley cell generated by IPSL-CM5A-LR model are close to those projected from CMIP5 dataset as listed in Table 1, thus the results derived from IPSL are not model-dependent. For instance, the location of maximum MSF in the Southern Hemisphere is (12.3° S, 700 hPa), in good agreement with simulation of BCC-CSM1-1, whereas maximal MSF in Northern Hemisphere is located in (14.2° N, 500 hPa) and are (almost) identical with NorESM1-M

CPD
9, 1449–1483, 2013

(FGOALS-S2) model in terms of latitudinal position as well as vertical position coincides well with MIROC-ESM model simulations.

4 Changes of Walker circulation in the RCP4.5 and mid-Pliocene compared to pre-industrial control run

Walker circulation is the most important large scale zonal overturning circulation in the tropics. It is characterized by rising air in the equatorial western Pacific, flowing eastward in the upper troposphere and sinking in the eastern Pacific, returning towards the western Pacific in the lower levels (Walker and Bliss, 1932, 1937). Changes in Walker circulation have large impact on the global and regional climate (Ropelewski and Halpert, 1989; Power et al., 1999; Holmgren et al., 2001). Thus it has been a major research focus for many years (Trenberth and Hoar, 1997; Collins et al., 2010; Sohn et al., 2012).

Figure 3a–c shows the Walker circulation defined by the divergent component of horizontal vector, corresponding potential velocity (contours) at 200 hPa and vertical weighted average of vertical wind ω over each grid cell at each level (from 100 hPa to 1000 hPa) weighted by the level's pressure depth (shaded dots), derived from the Control run, mid-Pliocene and RCP4.5 scenario, respectively. The annual mean Walker circulation is represented by ascending motion over the tropical western Pacific and descending motion over the eastern Pacific as displayed in Fig. 3a–c.

Walker circulation changes are first examined in the past warm climate and future scenario relative to the pre-industrial control run and the comparison between RCP4.5 simulation and mid-Pliocene modeling will be examined in detail in the next paragraph. Simulated mid-Pliocene Walker circulation is weakened compared to the pre-industrial control run, and is characterized by drastic decay of upward motion in the tropical western Pacific "warm pool" (90–150° E) and a decrease of upper level divergence in this region (Fig. 3d). Walker circulation in the RCP 4.5 scenario is also quite different from the control simulation, associated with a large weakening of ascending motion

CPD
9, 1449–1483, 2013

(90–120° E) to the west of divergent center and an increase of ascending motion (140–180° E) to the east of the maximal divergence. As a result, the rising branch of Walker in the future scenario is weakened in tropical western Pacific and shifted eastward (Fig. 3e). These behaviors of Walker cell in both warm climates depict clearly changes of Walker circulation in comparison with control run; nevertheless large differences of Walker cell responses exist between RCP4.5 and mid-Pliocene as shown in Fig. 3f. Ascending branch of Walker cell in future scenario is more decreased over the tropical western Pacific but an increase of divergence at 200 hPa takes place over the central Pacific, whereas these changes do not occur in the mid-Pliocene warm climate.

To display the vertical profile of Walker cell and quantify the ascending branch of Walker cell, we computed MSF-like indicator, defined as the vertical integration of the divergent component of zonal wind in low latitude (30° S–30° N) (Kamae et al., 2011), The positive values of MSF like represent net eastward divergent transport while the negative values indicate net westward divergent transport. There are two enclosed the zonal cell as displayed by Fig. 4a–c. One is the clockwise cell located over the Pacific and the other is anticlockwise, associated with the principal part over the Indian Ocean. The former is indeed Walker circulation over the Pacific Ocean (i.e. the characteristic of Walker cell can be captured by MSF-like indicator) and thus longitudinal position where MSF-like value equals zero at 500 hPa over the region (120° E–180) enables us to describe the differences of longitudinal position of the ascending branch of Walker cell between RCP4.5 scenario and mid-Pliocene (Fig. 4d). The ascending branch of Walker cell slightly shifts eastward in the mid-Pliocene warm climate (139.7° E) compared with the control run(138.5° E), while the longitudinal position of this ascending branch in the future scenario (156.2° E) shifts eastward much more than mid-Pliocene and control run, which is consistent with previous results from the divergent horizontal vector at 200 hPa (Fig. 3d–f).

To evaluate the robustness of our results, we also examine the Walker cell in RCP4.5 scenario derived from CMIP5 models. The weakening ascending motion over the western Pacific and increasing ascending motion over the central Pacific can be seen in the

CPD
9, 1449–1483, 2013

MPI-ESM-LR model and NorESM1-M model (not shown). Therefore, the behavior of Walker cell in future warm climate is robust.

5 Dynamical explanations of Hadley and Walker cell responses to both warm climate conditions

5.1 Hadley and Walker circulation changes in the RCP4.5 and mid-Pliocene in response to global warming

Observational analyses have demonstrated that the Hadley cell expanded poleward in recent decades (Hu and Fu, 2007) and various modeling studies have investigated the expansion of Hadley cell under global warming (Lu et al., 2007). Results suggested that climate models have the capability of modeling the observed poleward shift of Hadley cell, despite simulated expansion of Hadley cell in terms of magnitude is smaller than the observed values (Johanson and Fu, 2009). Recent modeling study suggested that increasing greenhouse gases plays an important role in causing the observed poleward expansion of Hadley circulation (Hu et al., 2013). Climate models predict a weakening of the atmospheric convective overturning in response to surface warming driven by increase in greenhouse gases (Knutson and Manabe, 1995; Tanaka et al., 2004; Held and Soden, 2006). Subsequent analysis argued weakening of tropical Pacific atmospheric circulation is due to anthropogenic forcing (Vecchi et al., 2006). Widening of Hadley cell and slow-down of Walker cell are detectable in both warm climates and whether these changes of Hadley and Walker cell in response to future and past global warming are related to the increasing atmospheric CO_2 concentration will be clarified in Sects. 5.2 and 5.3.

Both the observational analysis and numerical simulations suggest that the interannual variability of boreal winter Hadley cell is closely related to the ENSO phenomenon (Sun et al., 2012). Walker circulation is one of the most prominent atmospheric systems in the tropics and most of previous studies focused on the interannual variability of

CPD
9, 1449–1483, 2013

Walker circulation and its relationship with the ENSO activity (Power and Smith, 2007). Observational and modeling indicates that since mid-nineteenth century tropical SST has warmed 0.5–0.6 °C (Rayner et al., 2003; Knutson et al., 2006). As such, it has been emphasized that SST changes over tropical Pacific would have substantial influence on the variation of tropical atmospheric circulation, especially in Walker cell (Vecchi and Soden, 2007). However, SST changes in both simulations have many common features and exhibit very similar pattern compared to SST in the control run, despite the SST changes in RCP4.5 scenario are larger than mid-Pliocene warm climate (Fig. 5). Therefore, SST changes in both warm climates perhaps could not explain so large differences of Walker cell responses between RCP4.5 scenario and mid-Pliocene. Indeed, the detailed response of Hadley and Walker cell to increasing greenhouse gases is complex, as Hadley and Walker cell are influenced by many factors. In this study, we attempt to give the explanation of the Hadley cell and Walker circulation changes from the perspective of atmospheric dynamics.

5.2 Dynamical mechanism of Hadley cell response to global warming

In theory, both the Hadley and Walker cells are directly driven by the south-north and east-west thermal contrast, respectively. It means that Hadley cell is directly driven by zonal average equator-to-pole pressure gradient in the upper troposphere, which is largely determined by zonal average temperature gradient from equator to pole in upper troposphere (Webster, 2004). As shown in Fig. 6a–b, tropospheric warming has not been globally uniform in both warm climates with maximal center in the tropical upper troposphere and this non-uniform warming would lead to an increase of poleward air temperature gradient in future scenario and past warm climate (Fig. 6a–b). Increase of equator-to-pole temperature gradient is responsible for increasing poleward pressure gradient (Fig. 6c–d) and thereby be beneficial for the poleward expansion of Hadley cell simulated by future scenario and mid-Pliocene warm period. Moreover, meridional air temperature gradient increases more in the RCP4.5 scenario in terms of magnitude than in the mid-Pliocene climate (Fig. 6e), which would lead to a larger poleward

CPD
9, 1449–1483, 2013

pressure gradient in the RCP4.5 than mid-Pliocene (Fig. 6f) and thus could explain larger expansion of Hadley cell in RCP4.5 scenario than in the mid-Pliocene.

In brief, the non-uniform warming in the troposphere would be the crucial cause of poleward expansion of Hadley cell in the mid-Pliocene and future scenario. One important question is what caused the non-uniform warming in the troposphere? Recent modeling studies argued that anthropogenic CO_2 increases plays an important role in widening of observed Hadley circulation (Hu et al., 2013). In the present study, we consider that CO_2 concentration increasing would be possible factors responsible for non-uniform warming in both warm climates. Indeed, the magnitude of this non-uniform warming increase with CO_2 concentration, which could explain poleward expansion of Hadley cell in RCP4.5 scenario (543 ppm) and mid-Pliocene (405 ppm) compared to the pre-industrial run (280 ppm) and larger widening of Hadley cell in future scenario (543 ppm) than mid-Pliocene (405 ppm).

5.3 Dynamical mechanism of Walker circulation response to global warming

We first examine the annual mean west/east thermal contrast over the tropical upper level troposphere. Figure 7 represents the 400–100 millibar average air temperature and potential height along 20° S–20° N derived from the three different simulations. The annual average air temperatures derived from the three experiments exhibit a number of common features (Fig. 7a–c): there are three significant peaks of annual mean air temperature associated with three significant valleys and most prominent peak and valley are over the tropical western and eastern Pacific, respectively. As a result, the west-to-east air temperature gradient is established over the tropical Pacific, which directly leads to the west-to-east pressure gradient formation over the Pacific for the three simulations (Fig. 7d–f) and thereby directly driving the airflow eastward over the western Pacific and cooling sinks over the eastern tropical Pacific.

Non-uniform zonal atmospheric warming explains the different behaviors of the Walker circulation between RCP4.5 scenario and mid-Pliocene warm period. Most significant warming occurs in the mid-Pliocene to the west of annual average maximum

CPD
9, 1449–1483, 2013

of control run with reversed air temperature gradient generated from Indian Ocean to western Pacific (Fig. 8a), leading to pressure gradient from Indian Ocean to western Pacific (Fig. 8b) and thereby suppressing upper-level divergence and thus weakening the ascending branch of Walker cell over the western Pacific during mid-Pliocene. Projected warming features two significant peaks located in the west and east sides of the present day maximum of air temperature, respectively, associated with two valleys confined over the tropical western and eastern Pacific, respectively. Therefore, there are two reversed air temperature gradients generated over the tropical western Pacific compared with present day condition and both are directed to the tropical western Pacific, whereas two reversed temperature gradient dominate the central Pacific and the first is from central to western Pacific and the second is from central to eastern Pacific (Fig. 8c). The former temperature gradient leads to central-to-western Pacific pressure gradient and directly suppresses the ascending motion of the Walker circulation over the western Pacific, while the latter one leads to the pressure gradient from western to eastern Pacific and thereby increases the divergence over the central Pacific (Fig. 8d). The response of the pressure gradient to the non-uniform warming exhibits large differences between RCP4.5 and mid-Pliocene (Fig. 8e–f), which would be responsible for the differences of the Walker cell between both simulations.

Non-uniform atmospheric warming in response to the increasing CO_2 concentration changes the meridional and zonal thermal contrasts for both simulations and thus largely drives the extent of Hadley cell and the strength of Walker circulation in the mid-Pliocene and RCP4.5 scenario.

6 The impact of Hadley and Walker circulation on regional hydrological cycle

In this section, we will examine the response of hydrological cycle associated with Hadley cell and Walker circulation under global warming scenario. Figure 9a–c shows simulated annual mean precipitation for the three different experiments (pre-industrial control run, mid-Pliocene and RCP4.5 scenario). Spatial patterns of precipitation

CPD
9, 1449–1483, 2013

distribution have large similarities, characterized with increased rainfall in the tropics and middle latitude ocean but decreased precipitation in the subtropics and higher latitudes. Double ITCZ phenomenon is still depicted in the coupled model simulations.

It is well known that the subtropics experience relatively lower levels of precipitation due to subsidence of the Hadley circulation. As suggested in Sect. 3, the strength of Hadley cell increases remarkably in the subtropics and the edge-latitudes of Hadley cell boundaries shift poleward in both warm climates, which lead to much drier subtropical regions and poleward expansion of the edges of subtropical dry zone, respectively (Fig. 9d–e). The subtropics in both hemispheres are much drier in the future scenario than the mid-Pliocene, which is consistent with stronger Hadley cell in the subtropics and larger expansion of Hadley cell boundaries by comparing future scenario with past warm climate (Fig. 9f).

Tropical precipitation experiences significant changes in both simulations compared to the control run. Decrease of the precipitation over the western equatorial Pacific coincides with the slow-down of Walker cell in the mid-Pliocene, whereas increase of the precipitation over the central Pacific is consistent with the ascending branch of Walker cell shifting eastward from western Pacific to central Pacific in the future simulation.

7 Discussion and conclusion

In this paper, we investigated the changes of Hadley and Walker circulations in the mid-Pliocene and future warm climates based on the comparison with the pre-industrial control experiment. We analyze the response of Hadley and Walker cells in both contexts of warm climates and explained most of the changes occurring in the tropics through large scale atmospheric dynamics. The main conclusions are as follows.

There are many similarities in Hadley cell response to both warm climates. i.e. the strength of Hadley cell shows obvious intensification in both subtropics and a decrease in the northern tropics. The intensified Hadley cells in both subtropics lead to widening

CPD
9, 1449–1483, 2013

of Hadley cell boundaries in both warm climates. Moreover, the poleward expansion of Hadley cell is larger in RCP4.5 scenario than mid-Pliocene, which is very consistent with the higher CO_2 concentration (543 ppm) in future scenario than mid-Pliocene (405 ppm).

Simulated Walker cell exhibits many similarities for both climates but also depicts some differences between mid-Pliocene and RCP4.5 scenario. For instance, the ascending branch of Walker cell is suppressed over the western tropical Pacific compared to the present day, leading to a slow-down Walker cell and suppression of precipitation over the western Pacific in both simulations. The major difference of Walker cell responses is that the ascending branch of Walker cell in RCP4.5 scenario is shifted eastward while this does not happen in mid-Pliocene. The response of west-to-east thermal contrast exhibits large differences between RCP4.5 and mid-Pliocene, which could explain the differences of the Walker cell between both simulations.

Indeed, south-to-north thermal contrast increases linearly with CO_2 concentration and thereby Hadley cell in mid-Pliocene is a good analogue for projected Hadley cell, whereas the response of west-to-east thermal contrast to CO_2 increasing concentration is not similar which implies some limits to the analogue hypothesis.

Multi-model comparative studies have been performed on the Hadley and Walker cells in the future climate and results suggested that the widening of Hadley cell and weakening of ascending branch of Walker cell over western Pacific and increase divergence over central Pacific are robust features i.e. not model-dependent. Our results demonstrate that simulated Walker cell generally slows down and Hadley cells expand poleward in the mid-Pliocene warm climate, which are consistent with most recent modeling studies (Kamae et al., 2011). Moreover, this paper mainly focuses on the model comparison of past and future warm climate. An interesting issue would indeed beyond our investigation whether the weakening rise motion of Walker cell is relevant to the "permanent El Niño-like" condition in mid-Pliocene.

Acknowledgements. We thank JOINT DOCTORAL PROMOTION PROGRAMME (DPP) between Chinese Academy of Sciences (CAS) and Centre National de la Recherche Scientifique

CPD
9, 1449–1483, 2013

(CNRS), and CAS for providing financial support for my one year visit. Thanks also to Yan Zhao (LSCE/IPSL, CEA-CNRS-UVSQ, Gif-sur-Yvette, France) for comments on an earlier version of this manuscript.

The publication of this article is financed by CNRS-INSU.

References

Bragg, F. J., Lunt, D. J., and Haywood, A. M.: Mid-Pliocene climate modelled using the UK Hadley Centre Model: PlioMIP Experiments 1 and 2, Geosci. Model Dev., 5, 1109–1125, doi:10.5194/gmd-5-1109-2012, 2012.

Collins, M., An, S.-I., Cai, W., Ganachaud, A., Guilyardi, E., Jin, F.-F., Jochum, M., Lengaigne, M., Power, S., Timmermann, A., Vecchi, G., and Wittenberg, A.: The impact of global warming on the tropical Pacific Ocean and El Nino, Nat. Geosci., 3, 391–397, 2010.

Contoux, C., Ramstein, G., and Jost, A.: Modelling the mid-Pliocene Warm Period climate with the IPSL coupled model and its atmospheric component LMDZ5A, Geosci. Model Dev., 5, 903–917, doi:10.5194/gmd-5-903-2012, 2012.

Crowley, T. J.: Pliocene climates: the nature of the problem, Mar. Micropaleontol., 27, 3–12,1996.

Dowsett, H. J.: Global warming analysis-PRISM 3D, USGS, available at: http://geology.er.usgs.gov/eespteam/prism/prism3main.html, 2006.

Dowsett, H. J. and Robinson, M. M: Mid-Pliocene equatorial Pacific sea surface temperature reconstruction: a multi-proxy perspective, Phil. Trans. R. Soc. A., 367, 109–125, 2009.

Dowsett, H. J., Cronin, T. M., Poore, R. Z., Thompson, R. S., Whatley, R. C., and Wood, A. M: Micropaleontological Evidence for Increased Meridional Heat Transport in the North Atlantic Ocean During the Pliocene, Science, 258, 1133–1135, 1992.

CPD
9, 1449–1483, 2013

Dowsett, H., Barron, J., and Poore, R: Middle Pliocene sea surface temperatures: a global reconstruction, Mar. Micropaleontol., 27, 13–25, 1996.
Dowsett, H. J., Barron, J. A., Poore, R. Z., Thompson, R. S., Cronin, T. M., Ishman, S. E., and Willard, D. A: Middle Pliocene paleoenvironmental reconstruction: PRISM2. USGS, open file report, 99–535, available at: http://pubs.usgs.gov/openfile/of99-535, 1999.
Dufresne, J.-L., Foujols, M.-A., Denvil, S., Caubel, A., Marti, O., Aumont, O. Balkanski, Y., Bekki, S., Bellenger, H., Benshila, R., Bony, S., Bopp, L., Braconnot, P., Brockmann, P., Cadule, P., Cheruy, F., Codron, F., Cozic, A., Cugnet, D., de Noblet, N., Duvel, J.-P., Ethé, C., Fairhead, L., Fichefet, T., Flavoni, S., Friedlingstein, P., Grandpeix, J.-Y., Guez, L., Guilyardi, E., Hauglustaine, D., Hourdin, F., Idelkadi, A., Ghattas, J., Joussaume, S., Kageyama, M., Krinner, G., Labetoulle, S., Lahellec, A., Lefebvre, M.-P., Lefevre, F., Levy, C., Li, Z. X., Lloyd, J., Lott, F., Madec, G., Mancip, M., Marchand, M., Masson, S., Meurdesoif, Y., Mignot, J., Musat, I., Parouty, S., Polcher, J., Rio, C., Schulz, M., Swingedouw, D., Szopa, S., Talandier, C., Terray, P., and Viovy, N: climate change projections using the ISPL-CM5 earth system model: from CMIP3 to CMIP5, Clim. Dynam., doi:10.1007/s00382-012-1636-1, in press, 2012.
Fichefet, T. and Maqueda, M. A. M.: Sensitivity of a global sea ice model to the treatment of ice thermodynamics and dynamics, J. Geophys. Res., 102, 12609–12646, 1997.
Foster, G. L., Lunt, D. J., and Parrish, R. R.: Mountain uplift and the glaciation of North America – a sensitivity study, Clim. Past, 6, 707–717, doi:10.5194/cp-6-707-2010, 2010.
Haywood, A. M. and Valdes, P. J.: Modelling Pliocene warmth: contribution of atmosphere, oceans and cryosphere, Earth Planet. Sci. Lett., 218, 363–377, 2004.
Haywood, A. M., Valdes, P. J., and Sellwood, B. W.: Global scale palaeoclimate reconstruction of the middle Pliocene climate using the UKMO GCM: initial results, Global Planet. Change, 25, 239–256, 2000.
Haywood, A. M., Dowsett, H. J., Otto-Bliesner, B., Chandler, M. A., Dolan, A. M., Hill, D. J., Lunt, D. J., Robinson, M. M., Rosenbloom, N., Salzmann, U., and Sohl, L. E.: Pliocene Model Intercomparison Project (PlioMIP): experimental design and boundary conditions (Experiment 1), Geosci. Model Dev., 3, 227–242, doi:10.5194/gmd-3-227-2010, 2010.
Haywood, A. M., Dowsett, H. J., Robinson, M. M., Stoll, D. K., Dolan, A. M., Lunt, D. J., Otto-Bliesner, B., and Chandler, M. A.: Pliocene Model Intercomparison Project (PlioMIP): experimental design and boundary conditions (Experiment 2), Geosci. Model Dev., 4, 571–577, doi:10.5194/gmd-4-571-2011, 2011.

CPD
9, 1449–1483, 2013

Haywood, A. M., Hill, D. J., Dolan, A. M., Otto-Bliesner, B. L., Bragg, F., Chan, W.-L., Chandler, M. A., Contoux, C., Dowsett, H. J., Jost, A., Kamae, Y., Lohmann, G., Lunt, D. J., Abe-Ouchi, A., Pickering, S. J., Ramstein, G., Rosenbloom, N. A., Salzmann, U., Sohl, L., Stepanek, C., Ueda, H., Yan, Q., and Zhang, Z.: Large-scale features of Pliocene climate: results from the Pliocene Model Intercomparison Project, Clim. Past, 9, 191–209, doi:10.5194/cp-9-191-2013, 2013.

Held, I. M. and Soden, B. J.: Robust Responses of the Hydrological Cycle to Global Warming, J. Climte, 19, 5686–5699, 2006.

Holmgren, M., Scheffer, M., Ezcurra, E., Gutiérrez, J. R., and Mohren, G. M. J.: El Niño effects on the dynamics of terrestrial ecosystems, Trends Ecol. Evolut., 16, 89–94, 2001.

Houghton, J. T., Ding, Y., Griggs, D. J., Noguer, M., van der Linden, P. J., Dai, X., Maskell, K., and Johnson, C. A.: Climate Change 2001: The Scientific Basis. Contribution of Working Group I to the Third Assessment Report of the Intergovernmental Panel on Climate Change, Cambridge University Press, Cambridge, United Kingdom and New York, NY, USA, 881 pp., 2001.

Hourdin, F., Foujols, M.-A., Codron, F., Guemas, V., Dufresne, J.-L., Bony, S., Denvil, S., Guez, L., Lott, F., Ghattas, J., Braconnot, P., Marti, O., Meurdesoif, Y., and Bopp, L.: Climate and sensitivity of the IPSL-CM5A coupled model: impact of the LMDZ atmospheric grid configuration, Clim. Dynam., doi:10.1007/s00382-012-1411-3, in press, 2013.

Hu, Y. and Fu, Q.: Observed poleward expansion of the Hadley circulation since 1979, Atmos. Chem. Phys., 7, 5229–5236, doi:10.5194/acp-7-5229-2007, 2007.

Hu, Y., Tao, L., and Liu, J.: Poleward expansion of the Hadley circulation in CMIP5 simulations, Adv. Atmos. Sci., in press, 2013.

Jakobsson, M., Backman, J., Rudels, B., Nycander, J., Frank, M., Mayer, L., Jokat, W., Sangiorgi, F., O/'Regan, M., Brinkhuis, H., King, J., and Moran, K.: The early Miocene onset of a ventilated circulation regime in the Arctic Ocean, Nature, 447, 986–990, 2007.

Jansen, E., Overpeck, J., Briffa, K. R., Duplessy, J.-C., Joos, F., Masson-Delmotte, V., Olago, D., Otto-Bliesner, B., Peltier, W. R., Rahmstorf, S., Ramesh, R., Raynaud, D., Rind, D., Solomina, O., Villalba, R., and Zhang, D.: Palaeoclimate, in: Climate Change 2007: The Physical Science Basis. Contribution of Working Group I to the Fourth Assessment Report of the Intergovernmental Panel on Climate Change, edited by: Solomon, S., Qin, D., Manning, M., Chen, Z., Marquis, M., Averyt, K. B., Tignor, M., and Miller, H. L., Cambridge University Press, Cambridge, United Kingdom and New York, NY, USA, 2007.

CPD
9, 1449–1483, 2013

Johanson, C. M. and Fu, Q.: Hadley Cell Widening: Model Simulations versus Observations, J. Climate, 22, 2713–2725, 2009.
Kamae, Y. and Ueda, H.: Mid-Pliocene global climate simulation with MRI-CGCM2.3: set-up and initial results of PlioMIP Experiments 1 and 2, Geosci. Model Dev., 5, 793–808, doi:10.5194/gmd-5-793-2012, 2012.
Kamae, Y., Ueda, H., and Kitoh, A.: Hadley and Walker Circulations in the Mid-Pliocene Warm Period Simulated by an Atmospheric General Circulation Model, J. Meteor. Soc. Jpn., 89, 475–493, 2011.
Knutson, T. R. and Manabe, S.: Time-Mean Response over the Tropical Pacific to Increased C02 in a Coupled Ocean-Atmosphere Model, J. Climate, 8, 2181–2199, 1995.
Knutson, T. R., Delworth, T. L., Dixon, K. W., Held, I. M., Lu, J., Ramaswamy, V., Schwarzkopf, M. D., Stenchikov, G., and Stouffer, R. J.: Assessment of Twentieth-Century Regional Surface Temperature Trends Using the GFDL CM2 Coupled Models, J. Climate, 19, 1624–1651, 2006.
Krantz, D. E.: A chronology of Pliocene sea-level fluctuations: The U.S. Middle Atlantic Coastal Plain record, Quaternary Sci. Rev., 10, 163–174, 1991.
Krinner, G., Viovy, N., de Noblet-Ducoudré, N., Ogée, J., Polcher, J., Friedlingstein, P., Ciais, P., Sitch, S., and Prentice, I. C.: A dynamic global vegetation model for studies of the coupled atmosphere-biosphere system, Global Biogeochem. Cy., 19, GB1015, doi:10.1029/2003GB002199, 2005.
Lu, J., Vecchi, G. A., and Reichler, T.: Expansion of the Hadley cell under global warming, Geophys. Res. Lett., 34, L06805, doi:10.1029/2006GL028443, 2007.
Madec G: NEMO ocean engine, note du Pole de modelisation, Institut Pierre-Simon Laplace (IPSL), 2008.
Marti, O., Braconnot, P., Dufresne, J. L., Bellier, J., Benshila, R., Bony, S., Brockmann, P., Cadule, P., Caubel, A., Codron, F., Noblet, N., Denvil, S., Fairhead, L., Fichefet, T., Foujols, M. A., Friedlingstein, P., Goosse, H., Grandpeix, J. Y., Guilyardi, E., Hourdin, F., Idelkadi, A., Kageyama, M., Krinner, G., Lévy, C., Madec, G., Mignot, J., Musat, I., Swingedouw, D., and Talandier, C.: Key features of the IPSL ocean atmosphere model and its sensitivity to atmospheric resolution, Clim. Dynam., 34, 1–26, 2010.
Masson-Delmotte, V., Kageyama, M., Braconnot, P., Charbit, S., Krinner, G., Ritz, C., Guilyardi, E., Jouzel, J., Abe-Ouchi, A., Crucifix, M., Gladstone, R. M., Hewitt, C. D., Kitoh, A., LeGrande, A. N., Marti, O., Merkel, U., Motoi, T., Ohgaito, R., Otto-Bliesner, B., Peltier, W. R.,

CPD
9, 1449–1483, 2013

Ross, I., Valdes, P. J., Vettoretti, G., Weber, S. L., Wolk, F., and Yu, Y.: Past and future polar amplification of climate change: climate model intercomparisons and ice-core constraints, Clim. Dynam., 26, 513–529, 2006.

Miller, K. G., Wright, J. D., Browning, J. V., Kulpecz, A., Kominz, M., Naish, T. R., Cramer, B. S., Rosenthal, Y., Peltier, W. R., and Sosdian, S.: High tide of the warm Pliocene: Implications of global sea level for Antarctic deglaciation, Geology, 29, 1679–1715, 2012.

Oort, A. H. and Yienger, J. J.: Observed Interannual Variability in the Hadley Circulation and Its Connection to ENSO, J. Climate, 9, 2751–2767, 1996.

Power, S. B. and Smith, I. N.: Weakening of the Walker Circulation and apparent dominance of El Niño both reach record levels, but has ENSO really changed?, Geophys. Res. Lett., 34, L18702, doi:10.1029/2007GL030854, 2007.

Power, S. B., Casey, T., Folland, C., Colman, A., and Mehta, V.: Inter-decadal modulation of the impact of ENSO on Australia, Clim. Dynam., 15, 319–324, doi:10.1130/1052-5173(2006)016<4:EFENLC>2.0.CO;2, 1999.

Quan, X. W., Diaz, H. F., and Hoerling, M. P.: Changes in the tropical Hadley cell since 1950, in: Hadley Circulation: Present, Past and Future, edited by: Dias, H. F. and Bradley, R. S., Amsterdam: Springer, 85–120, 2004.

Ramstein, G., Serafini-Le Treut, Y., Le Treut, H., Forichon, M., and Joussaume, S.: Cloud processes associated with past and future climate changes, Clim. Dynam., 14, 233–247, 1998.

Raymo, M. E., Grant, B., Horowitz, M., and Rau, G. H.: Mid-Pliocene warmth: stronger greenhouse and stronger conveyor, Mar. Micropaleontol., 27, 313–326, 1996.

Ravelo, A. C., Dekens, P. S., and McCarthy, M.: Evidence for El Nino-like conditions during the Pliocene, GSA Today, 16, 4–11, 2006.

Rayner, N. A., Parker, D. E., Horton, E. B., Folland, C. K., Alexander, L. V., Rowell, D. P., Kent, E. C., and Kaplan, A.: Global analyses of sea surface temperature, sea ice, and night marine air temperature since the late nineteenth century, J. Geophys. Res. 108, 4407, doi:10.1029/2002JD002670, 2003.

Ropelewski, C. F. and Halpert, M. S.: Precipitation Patterns Associated with the High Index Phase of the Southern Oscillation, J. Climate, 2, 268–284, 1989.

Salzmann, U., Haywood, A. M., Lunt, D. J., Valdes, P. J., and Hill, D. J.: A new global biome reconstruction and data-model comparison for the Middle Pliocene, Global Ecol. Biogeogr., 17, 432–447, 2008.

CPD
9, 1449–1483, 2013

Sohn, B. J., Yeh, S.-W., Schmetz, J., and Song, H.-J.: Observational evidences of Walker circulation change over the last 30 years contrasting with GCM results, Clim. Dynam, 1–12, doi:10.1007/s00382-012-1484-z, 2012.
Stepanek, C. and Lohmann, G.: Modelling mid-Pliocene climate with COSMOS, Geosci. Model Dev., 5, 1221–1243, doi:10.5194/gmd-5-1221-2012, 2012.
Sun, Y., Zhou, T., and Zhang, L.: Observational analysis and numerical simulation of the interannual variability of the boreal winter Hadley circulation over the recent 30 years, Sci. China Earth Sci., 1–15, doi:10.1007/s11430-012-4497-x, 2012.
Tanaka, H. L., Ishizaki, N., and Kitoh, A.: Trend and interannual variability of Walker, monsoon and Hadley circulations defined by velocity potential in the upper troposphere, Tellus A, 56, 250–269, 2004.
Thompson, R. S. and Fleming, R. F.: Middle Pliocene vegetation: reconstructions, paleoclimatic inferences, and boundary conditions for climate modeling, Mar. Micropaleontol., 27, 27–49, 1996.
Trenberth, K. E. and Hoar, T. J.: El Niño and climate change, Geophys. Res. Lett., 24, 3057–3060, 1997.
Valcke S: OASIS3 user guide (prism_2-5), technical report TR/CMGC/06/73, PRISM Report No 2. CERFACS, Toulouse, p. 60, 2006.
Vecchi, G. A. and Soden, B. J.: Global Warming and the Weakening of the Tropical Circulation, J. Climate, 20, 4316–4340, 2007.
Vecchi, G. A., Soden, B. J., Wittenberg, A. T., Held, I. M., Leetmaa, A., and Harrison, M. J.: Weakening of tropical Pacific atmospheric circulation due to anthropogenic forcing, Nature, 441, 73–76, 2006.
Walker, G. T. and E. W. Bliss : World Weather V. Memo, Roy. Meteor. Soc., 4, 53–84, 1932.
Walker, G. T. and E. W. Bliss: World Weather VI. Memo. Roy. Meteor. Soc., 4, 119–139, 1937.
Wara, M. W., Ravelo, A. C., and Delaney, M. L.: Permanent El Niño-Like Conditions During the Pliocene Warm Period, Science, 309, 758–761, 2005.
Webster, J. P.: The elementary Hadley circulaiton, in: Hadley Circulation: Present, Past and Future, edited by: Dias, H. F. and Bradley, R. S., Amsterdam: Springer, 9–60, 2004.
Yan, Q., Zhang, Z.-S., and Gao,Y.-Q.: An East Asian monsoon in the mid-Pliocene, Atmos. Ocean. Sci. Lett., 5, 449–454, 2012.
Zhang, Z. and Yan, Q.: Pre-industrial and mid-Pliocene simulations with NorESM-L: AGCM simulations, Geosci. Model Dev., 5, 1033–1043, doi:10.5194/gmd-5-1033-2012, 2012.

CPD
9, 1449–1483, 2013

Zhang, Z. S., Nisancioglu, K., Bentsen, M., Tjiputra, J., Bethke, I., Yan, Q., Risebrobakken, B., Andersson, C., and Jansen, E.: Pre-industrial and mid-Pliocene simulations with NorESM-L, Geosci. Model Dev., 5, 523–533, doi:10.5194/gmd-5-523-2012, 2012.

CPD
9, 1449–1483, 2013

Table 1. Multi-model comparative analysis of Hadley circulaiton properties (maximum of MSF and corresponding position, Hadley cell boundaries) in the RCP4.5 scenario and Hadley cell boundaries from pre-industrial control run (bracket).

Model	Southern Maximum (10^{10} Kg s^{-1})	Hadley location	Cell edge	Northern Maximum (10^{10} Kg s^{-1})	Hadley location	Cell edge
IPSL-CM5A-LR	−10.07	(12.3° S, 700 hPa)	30.5° S (28.6° S)	6.93	(14.2° N, 500 hPa)	28.8° N (28.0° N)
MPI-ESM-LR	*-10.35*	(14.0° S, 700 hPa)	30.9° S (30.2° S)	7.*10*	(15.8° N,600 hPa)	*29.5° N* (29.0° N)
BCC-CSM1.1	−8.00	*(12.5° S, 700 hPa)*	31.1° S (30.3° S)	7.49	(15.4° N, 600 hPa)	*29.4° N* (28.9° N)
NorESM1-M	*−10.11*	(10.4° S, 700 hP)	33.4° S (32.6° S)	8.62	(*14.2° N*, 600 hPa)	30.8° N (30.5° N)
NCAR-CCSM4	−8.95	(13.7° S, 700 hP)	33.9° S (33.0° S)	7.23	(14.6° N, 600 hPa)	31.8° N (31.3° N)
FGOALS-S2	−8.33	(14.1° S, 700hP)	31.5° S (29.7° S)	7.33	(*14.1° N*, 600hPa)	*29.6° N* (28.5° N)
MIROC-ESM	−11.9	(9.8° S,700 hPa)	29.2° S (28.4° S)	8.74	(12.6° N, *500 hPa*)	27.9° N (27.7° N)

The italic represents the modeling consistency between IPSL model and other models.

CPD
9, 1449–1483, 2013

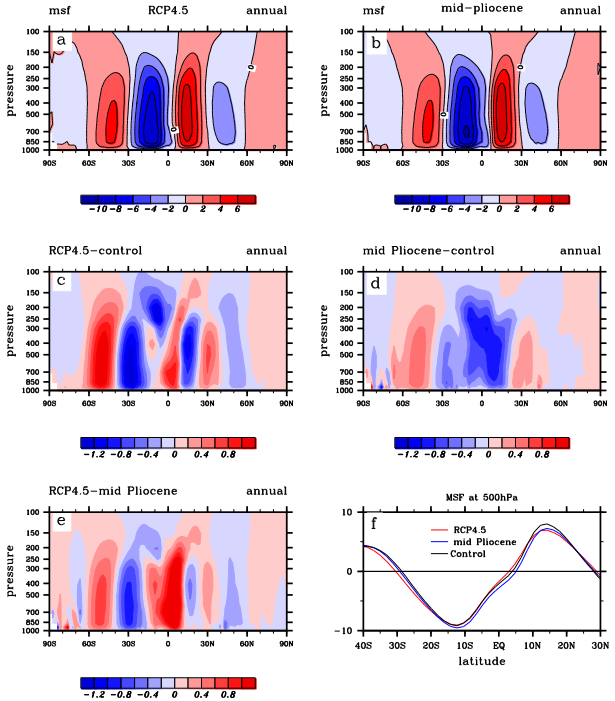

Fig. 1. Climatological annual average mass stream function (units: 10^{10} Kg s^{-1}) simulated by RCP4.5 **(a)** and mid-Pliocene **(b)**. Mass stream function changes in RCP4.5 and mid-Pliocene compared to the control run is displayed in **(c–d)**, respectively. Mass stream function difference between RCP4.5 and mid-Pliocene shown in **(e)** and **(f)** represents mass stream function at 500 hPa (red line: RCP4.5, blue line: mid-Pliocene, black line: Control run).

CPD
9, 1449–1483, 2013

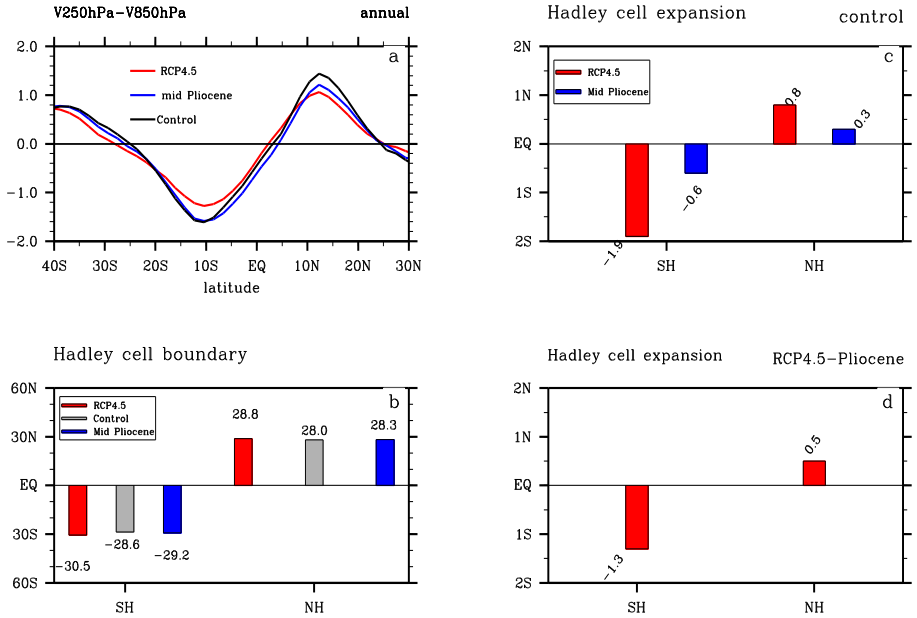

Fig. 2. (a) Simulated vertical shear of meridional wind (V250-V850) derived from three different simulations (Control run, RCP4.5 and mid-Pliocene). **(b)** Hadley cell edge in the three experiments. **(c)** Simulated Hadley cell expansion under two global warming periods. **(d)** Poleward shift of Hadley cell in the RCP4.5 scenario compared with the mid-Pliocene warm period.

CPD
9, 1449–1483, 2013

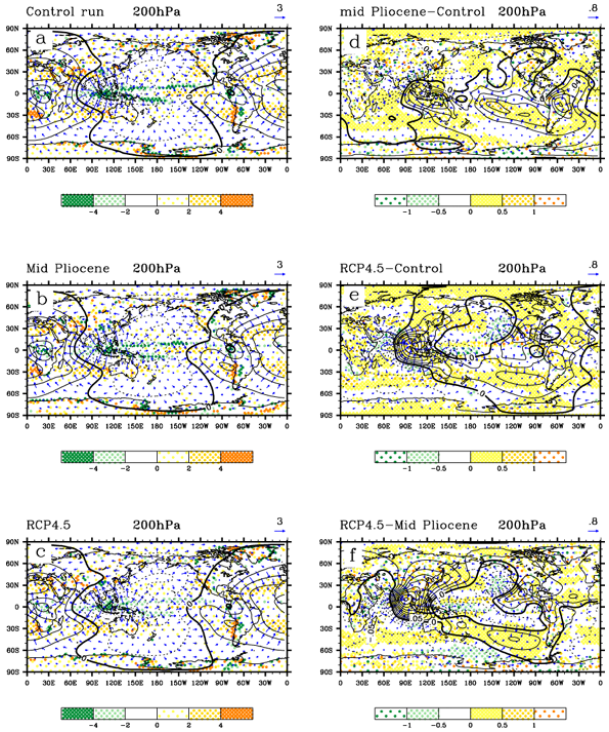

Fig. 3. Climatological annual average potential velocity (contours: $10^7\,m^2\,s^{-1}$) and divergent wind (blue vector; $m\,s^{-1}$) at 200-hPa height, vertically averaged vertical wind (ω, $10^{-2}\,m\,s^{-1}$) weighted by the level's pressure depth (shaded dot region), derived from different simulations: **(a)** pre-industrial control run; **(b)** mid-Pliocene warm period; **(c)** RCP4.5 scenario. The response of multi-variables (potential velocity, divergent, ω) to the future and mid-Pliocene warming relative pre-industrial run and comparative analysis of the RCP4.5 scenario and mid-Pliocene is displayed in **(d–f)**, respectively.

CPD
9, 1449–1483, 2013

A comparative study of large scale atmospheric circulation

Y. Sun et al.

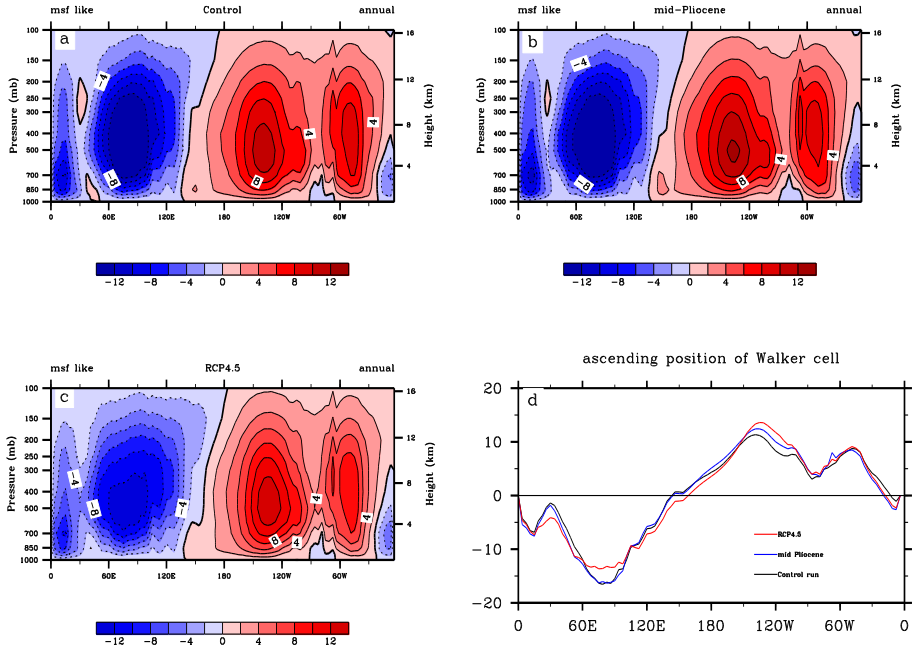

Fig. 4. MSF-like function (units: 10^{10} Kg s^{-1}) simulated by three different simulations (control run, mid Pliocene and RCP4.5 scenario) as displayed in **(a–c)**, respectively and MSF-like at 500 hPa used for description of longitudinal position of ascending branch of Walker cell **(d)**.

CPD
9, 1449–1483, 2013

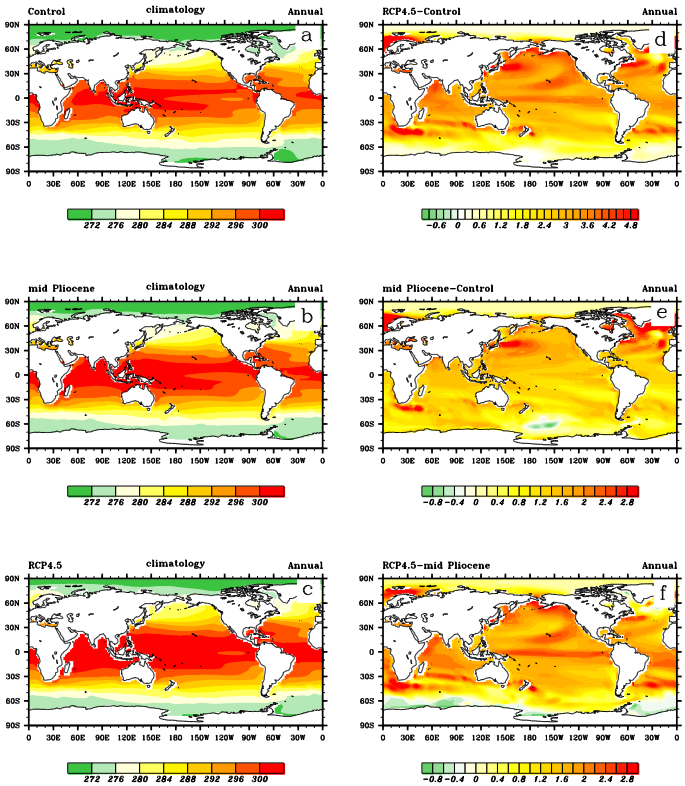

Fig. 5. Annual mean sea surface temperature (units: °C) in **(a)** pre-industrial control run, **(b)** mid-Pliocene and **(c)** RCP4.5. **(d)** Annual mean sea surface temperature anomalies between RCP4.5 and control run. **(e)** same as **(d)** between mid-Pliocene and control run. **(f)** same as **(e)** between RCP4.5 and mid-Pliocene.

CPD
9, 1449–1483, 2013

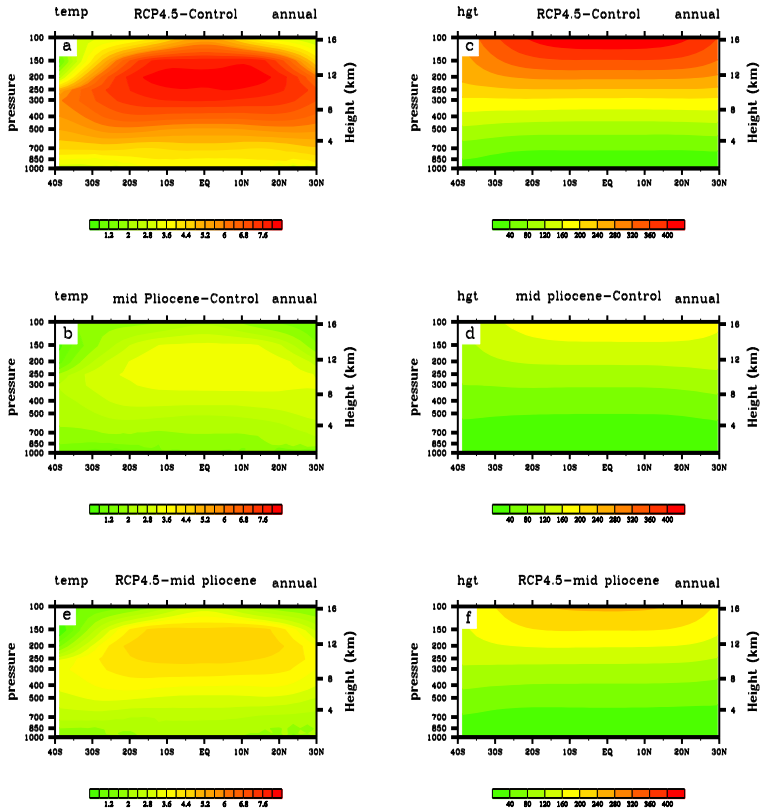

Fig. 6. (a) Zonal average air temperature anomalies between RCP4.5 and control run (units: °C). **(b)** same as **(a)** between mid-Pliocene and control run. **(c)** Potential height changes between RCP4.5 and control run (units: m). **(d)** same as **(c)** between mid-Pliocene and control run. **(e)** same as **(a)** between RCP4.5 and mid-Pliocene. **(f)** same as **(c)** between RCP4.5 and mid-Pliocene.

CPD
9, 1449–1483, 2013

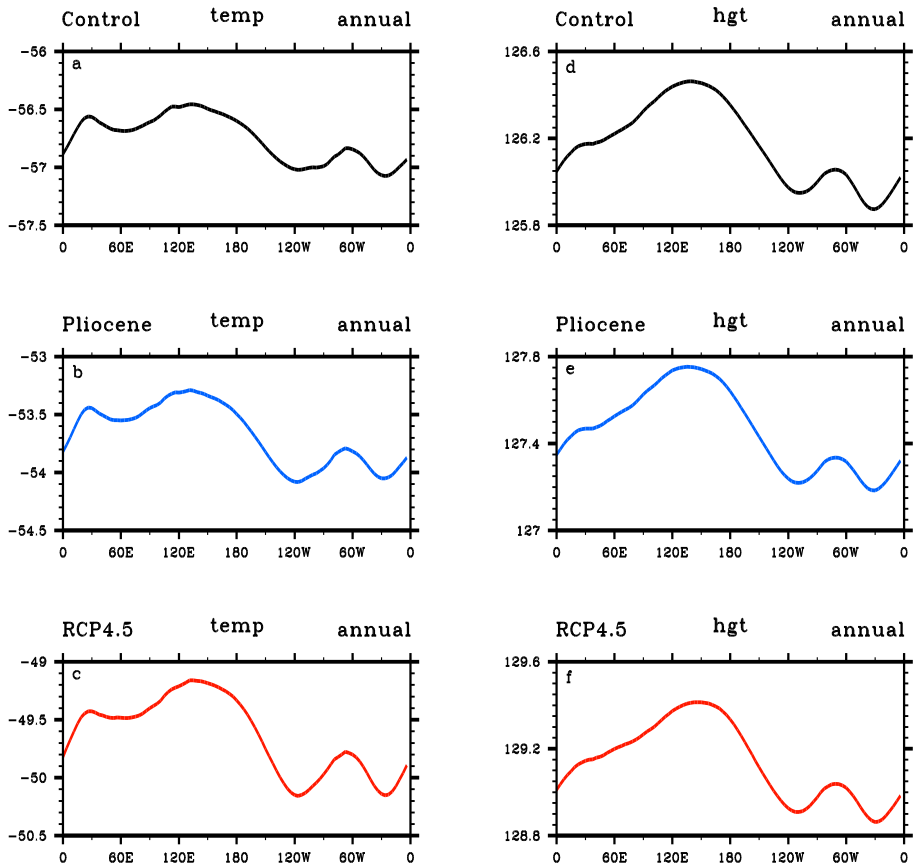

Fig. 7. Annual mean vertically averaged air temperature (° C) in the upper troposphere (400 hPa to 100 hPa) for **(a)** the control run, **(b)** mid Pliocene and **(c)** RCP4.5 scenario. Potential height (units: 10^2 m) for **(d)** the control run, **(e)** mid Pliocene and **(f)** RCP4.5 scenario.

CPD
9, 1449–1483, 2013

A comparative study of large scale atmospheric circulation

Y. Sun et al.

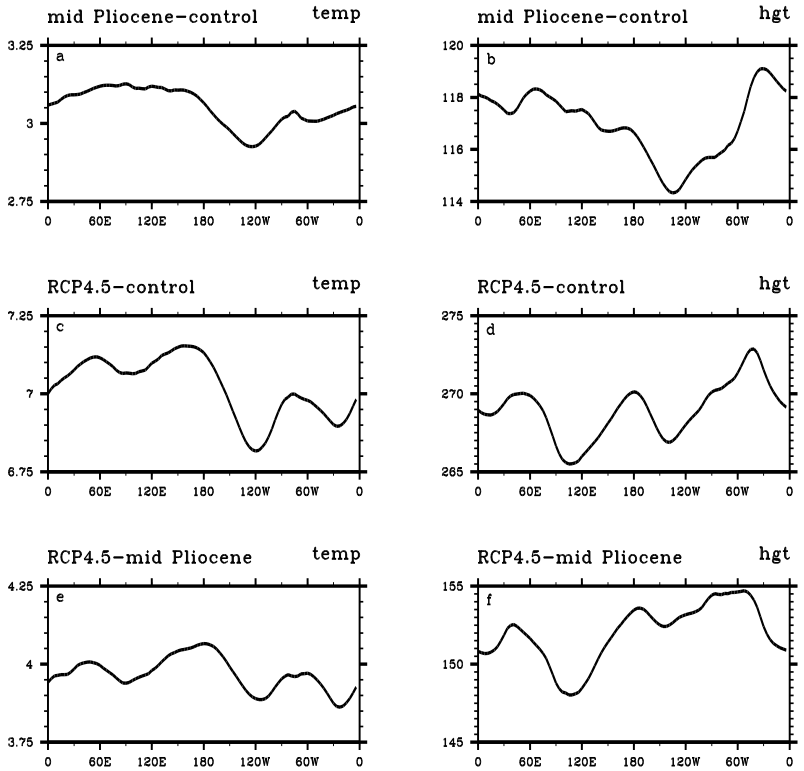

Fig. 8. (a) Vertically averaged upper level (from 400 hPa to 100 hPa) temperature anomaly (units: °C) between mid-Pliocene and control run. **(b)** Potential height anomaly (units: m) between mid-Pliocene and control run. **(c)** same as **(a)** between RCP4.5 and control run. **(d)** same as **(b)** between RCP4.5 and control run. **(e)** same as **(a)** between RCP4.5 and mid-Pliocene. **(f)** same as **(b)** between RCP4.5 and mid-Pliocene.

CPD
9, 1449–1483, 2013

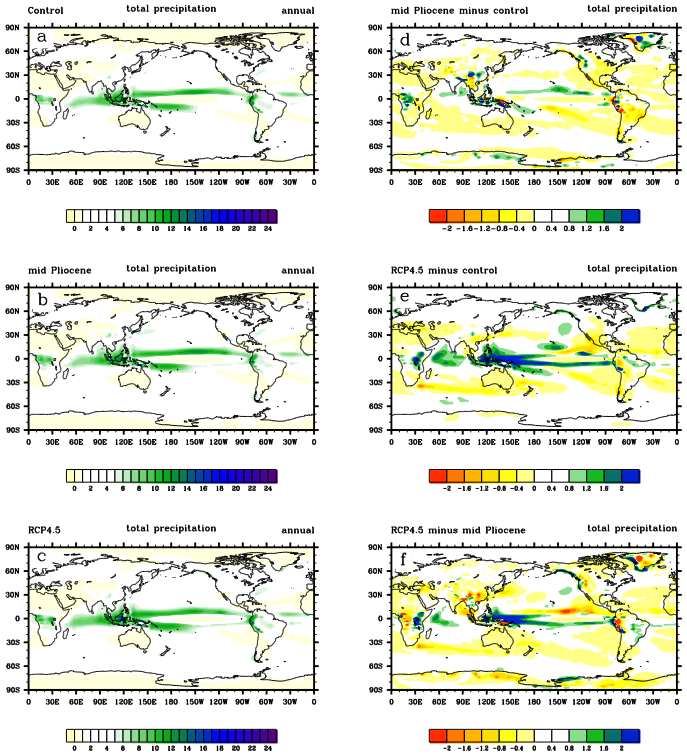

Fig. 9. Simulated annual mean total precipitation (units: mm day^{-1}) from the control run **(a)** mid-Pliocene period **(b)** and future scenario **(c)**. Simulated responses of the total precipitation to mid-Pliocene **(d)** and future warming climate **(e)** displayed in **(d–e)**, respectively. Simulated total precipitation difference between the RCP4.5 and mid-Pliocene shown in the **(f)**.

CPD
9, 1449–1483, 2013